Discharge-resolved erosion processes at the low-field side midplane of ASDEX Upgrade

J. Karhunen[1], M.I. Airila[1], A. Hakola[1], A. Herrmann[2], M. Mayer[2], H.W. Müller[2], R. Neu[2], V. Rohde[2], and the ASDEX Upgrade Team

[1] *VTT, Association Euratom-Tekes, P.O. Box 1000, FI-02044 VTT, Finland*

[2] *MPI für Plasmaphysik, EURATOM Association, D-85748 Garching, Germany*

Introduction

In future fusion reactors, the lifetime of plasma-facing components can be considerably restricted due to their large erosion or even melting in interactions with the plasma. The damage can be remarkable especially during H-mode operation, as ELMs expose the first wall to large particle and heat loads. Therefore, the choice of proper first-wall materials is essential to ensure the desired performance level of a reactor. [1]

This contribution concentrates on the erosion properties of W and other fusion-relevant materials in L- and H-mode plasmas at ASDEX Upgrade during its 2010–2011 experimental campaign. The experimentally determined erosion profiles of different marker materials have been compared with numerical predictions by the homogeneous material mixing model of the Monte Carlo code ERO [2].

Experiments

The experiments were carried out in ASDEX Upgrade in April 2011 using two graphite probes with 100-nm thick marker stripes of C and Al and 50-nm thick stripes of W and Ni, as shown in Figure 1. One of the probes was exposed to four identical L-mode discharges (shot numbers #26725–#26728) with the following parameters: $I_p = 1.0$ MA, $B_t = -2.73$ T, $P_{NBI} = 1.23$ MW, total $t_{flat\ top} = 14.8$ s. The second probe was exposed to a single H-mode discharge (#26748), with parameters $I_p = 0.80$ MA, $B_t = -2.48$ T, $P_{NBI} = 7.48$ MW, and $t_{flat\ top} = 1.1$ s. In both cases, the probes were in the scrape-off layer (SOL) plasma at the low-field side limiter region slightly above the midplane. The distance from the separatrix was 35 mm for the L-mode and 43 mm for the H-mode experiment.

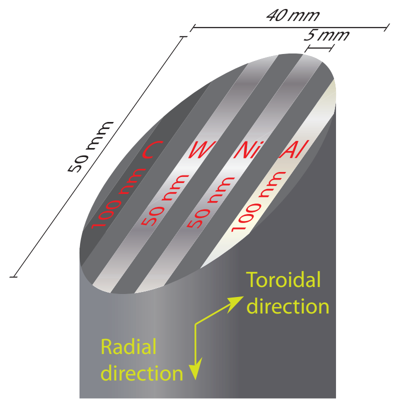

Figure 1: Schematic illustration of the probe head used in the experiments.

After the exposure, the marker stripes were analysed using Rutherford Backscattering Spectroscopy (RBS). For the L-mode probe, the RBS measurements were done using 3.0-MeV protons and 2.0-MeV alpha particles, whereas the H-mode probe was studied only with protons. The net erosion profile of each marker was determined by studying the resulting RBS spectra with the help of the program SIMNRA [3].

Simulations

Several ERO simulations were carried out to reproduce the experimentally observed erosion profiles. The simulations were run in a tracing box with radial, poloidal, and toroidal dimensions of 100 mm, 150 mm, and 150 mm, respectively. The probe head itself was modelled as a 50×50 mm^2 grid with a cell size of 2.5×2.5 mm^2. The marker stripes were 5 mm wide in poloidal direction and extended over the whole surface in toroidal direction. Since especially erosion of W is dominated by low-Z impurities, all simulations were run with a constant C^{4+} impurity concentration of 0.5%; here C represents all low-Z impurities such as B, O, N, and C itself. A somewhat realistic constant value was chosen, as no data for Z_{eff} was available. For W, sputtering and ionization data according to [4] and [5], respectively, were used.

Erosion of the plasma-facing components and transport of the test particles are defined by the background plasma for which the electron density, n_{e}, electron temperature, T_{e}, and ion temperature, T_{i}, were assumed to be of exponentially decaying form in the SOL. In the L-mode experiment, fitting to experimental data from the discharge #26728 resulted in the separatrix value and decay length of $n_{\mathrm{e0}} \approx 6.5 \times 10^{18}\ \frac{1}{\mathrm{m}^3}$ and $\lambda_{\mathrm{n_e}} \approx 37$ mm for n_{e}. For T_{e} and T_{i}, the corresponding values were varied within the ranges $T_{\mathrm{e0}} = 50 - 80$ eV, $T_{\mathrm{i0}} = 100 - 170$ eV, $\lambda_{\mathrm{T_e}} = 30 - 35$ mm, and $\lambda_{\mathrm{T_i}} = 30 - 40$ mm. The L-mode simulations consisted of 100 time steps with an overall simulation time of 16 s.

In H mode, ELMs were introduced as short time steps alternating with the inter-ELM phases. In the beginning of the simulations, an ELM-free period of 0.65 s was used, as indicated by the D_α data of the discharge #26748. After this, ELMs appeared periodically during 0.85 s such that the total simulation time was 1.5 s. The duration and frequency of ELMs was varied in the ranges $t_{\mathrm{ELM}} = 1 - 5$ ms and $f_{\mathrm{ELM}} = 50 - 250$ Hz.

Due to the ELMs, two separate background plasmas with different T_{e} and T_{i} had to be defined. For both of these, the exponential fit resulted in $n_{\mathrm{e0}} \approx 2.7 \times 10^{19}\ \frac{1}{\mathrm{m}^3}$ and $\lambda_{\mathrm{n_e}} \approx 21$ mm for the separatrix value and decay length of n_{e}, respectively. Varying the ELM and inter-ELM temperatures was not found to affect noticeably the observed erosion. Realistic values of $T_{\mathrm{e0,inter}} = 200$ eV, $\lambda_{\mathrm{T_e,inter}} \approx 21$ mm, $T_{\mathrm{i0,inter}} = 255$ eV, $\lambda_{\mathrm{T_i,inter}} \approx 38$ mm, $T_{\mathrm{e0,ELM}} = 350$ eV, $\lambda_{\mathrm{T_e,ELM}} \approx 30$ mm, $T_{\mathrm{i0,ELM}} = 400$ eV, and $\lambda_{\mathrm{T_i,ELM}} \approx 36$ mm were thus chosen, as they fitted reasonably well into the experimental data. No measurement data of T_{i} was available, thus, instead of using exponential fits, the values were estimated according to previous studies in [6].

Results

In L mode, the best match between experiments and simulations is obtained using rather low temperatures and long decay lengths. This can be seen in Figure 2 i), where the green curves correspond to the case of $T_{e0} = 60$ eV, $\lambda_{T_e} = 30$ mm, $T_{i0} = 150$ eV, and $\lambda_{T_i} = 30$ mm. These results match well with the experimentally observed erosion profiles of W and Ni, excluding the region closest to the plasma ($x > 40$ mm), where especially in the case of Ni the simulated erosion is too high. In the case of C, the simulations slightly overestimate erosion but for Al, the mismatch is significant everywhere across the probe. This can most likely be due to experimental uncertainties concerning the oxidation of Al; no proper cross-section data exists for Al oxides in SIMNRA for the 3.0-MeV protons and 2.0-MeV alpha particles.

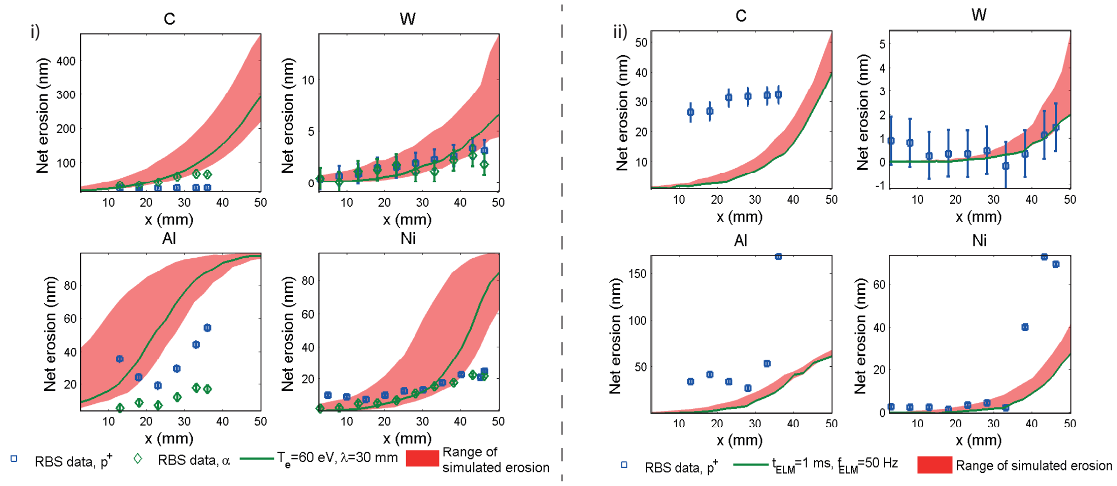

Figure 2: Erosion profiles of the marker materials in i) L mode and ii) H mode as functions of the distance along the probe surface. The x coordinate increases towards the plasma, the separatrix being at i) $x = 85$ or ii) $x = 93$.

The red area in Figure 2 i) represents the range of simulated net erosion that was covered by varying T_e and T_i and their decay lengths. Basically, it was found that high temperatures and long decay lengths induce more erosion than low temperatures and short decay lengths. In addition, the effect of T_e on erosion was noticed to be more significant than that of T_i, which was expectable especially in the presence of impurities, since the energy of impinging ions is given by $E = 2k_B T_i + 3Zk_B T_e$.

In H mode, erosion of C and Al could not be explained by the simulations, as can be seen in Figure 2 ii). This is most probably due to experimental uncertainties: RBS measurements with protons are unreliable for light elements, especially for C that can be distinguished from the graphite substrate only by studying the RBS spectrum of a thin layer of W between the substrate and the C marker stripe. For Al, also same uncertainties with the cross-section data apply as in the L-mode case. According to surface temperature data from an infrared camera, the Al layer is likely to have melted at the tip of the probe, which explains the steep rise of the experimental erosion profile.

In contrast, good results are observed for W and Ni, although erosion of nickel is heavily underestimated at the tip of the probe. The most realistic case of $t_{\mathrm{ELM}} = 1$ ms, $f_{\mathrm{ELM}} = 50$ Hz that corresponds most accurately to the D_α data of the discharge #26748 is indicated as a green line in the figure. The steep rise in the experimental erosion profile of Ni may again be due to melting, but the IR camera data was insufficient to confirm that.

According to the simulations, only the total duration of ELMs affected the results independently of the duration and frequency of ELMs, which suggests that redeposition was insignificant. With noticeable redeposition, changes in surface composition during long inter-ELM phases would have lead to larger erosion of deposited layers during ELMs than with shorter ELM cycles. Hence, the evolution of the surface would be different. This was observed also experimentally: only slight amounts of marker materials were found between the stripes. With realistic ratios of t_{ELM} and t_{inter} the inter-ELM periods were observed to yield larger erosion than ELMs. For W, ELMs began dominating erosion only after t_{ELM} was more than 20% of the duration of the ELM cycle, and even more unrealistic ratios were needed for other materials.

Conclusions

Erosion properties of fusion-relevant materials were studied at the low-field side limiter region of ASDEX Upgrade during the 2010–2011 experimental campaign. Two graphite probes with C, Al, W, and Ni markers were exposed to plasma during both L and H mode discharges, and ERO simulations were carried out to explain the observed erosion.

In L mode, erosion of W and, to some degree, also C and Ni could be reproduced using rather low electron and ion temperatures and longish decay lengths. In the case of aluminium, simulated erosion is overestimated; this is most probably due to experimental uncertainties.

Erosion of C and Al could not be explained with the H-mode simulations — again probably due to experimental uncertainties and the probable melting of Al. On the other hand, W and Ni show a good match throughout the simulation range — including the case $t_{\mathrm{ELM}} = 1$ ms, $f_{\mathrm{ELM}} = 50$ Hz that corresponds most accurately to experimental data — except for Ni at the tip of the probe, where melting may have occurred.

This work was carried out within the framework of the ITER Physics Support Activities.

The ERO code is maintained by Forschungszentrum Jülich.

References

[1] R.A. Pitts et al., Plasma Physics and Controlled Fusion **47** (2005) B303–B322

[2] A. Kirschner et al., Nuclear Fusion **40** (2000) 989–1001

[3] M. Mayer, *SIMNRA User's Guide*, available at `www.simnra.com`

[4] V.A. Abramov et al., Journal of Nuclear Materials **162–164** (1989) 462

[5] K.L. Bell et al., Rep. CLM-R216 (1982)

[6] M. Kočan et al., Nuclear Fusion **52** (2012) 023016